




The improvement of Mo/4H-SiC Schottky diodes via a P₂O₅ surface passivation treatment

Cite as: J. Appl. Phys. **127**, 025704 (2020); <https://doi.org/10.1063/1.5133739>

Submitted: 25 October 2019 . Accepted: 29 December 2019 . Published Online: 10 January 2020

A. B. Renz , V. A. Shah, O. J. Vavasour , Y. Bonyadi, F. Li, T. Dai, G. W. C. Baker, S. Hindmarsh, Y. Han, M. Walker, Y. Sharma, Y. Liu, B. Raghothamachar, M. Dudley, P. A. Mawby , and P. M. Gammon



View Online



Export Citation



CrossMark

ARTICLES YOU MAY BE INTERESTED IN

[Reduction of threading dislocation density in top-down fabricated GaN nanocolumns via their lateral overgrowth by MOCVD](#)

Journal of Applied Physics **127**, 025306 (2020); <https://doi.org/10.1063/1.5110602>

[Electronic states and interband tunneling conditions in type-II quantum well heterostructures](#)

Journal of Applied Physics **127**, 025705 (2020); <https://doi.org/10.1063/1.5133801>

[Understanding and optimizing EBIC pn-junction characterization from modeling insights](#)

Journal of Applied Physics **127**, 024502 (2020); <https://doi.org/10.1063/1.5139894>

Lock-in Amplifiers
Find out more today



Zurich Instruments



The improvement of Mo/4H-SiC Schottky diodes via a P₂O₅ surface passivation treatment

Cite as: J. Appl. Phys. 127, 025704 (2020); doi: 10.1063/1.5133739

Submitted: 25 October 2019 · Accepted: 29 December 2019 ·

Published Online: 10 January 2020






View Online



Export Citation



CrossMark

A. B. Renz,^{1,a)}  V. A. Shah,¹ O. J. Vavasour,¹  Y. Bonyadi,¹ F. Li,¹ T. Dai,¹ G. W. C. Baker,¹ S. Hindmarsh,² Y. Han,² M. Walker,² Y. Sharma,³ Y. Liu,⁴ B. Raghothamachar,⁴ M. Dudley,⁴ P. A. Mawby,¹  and P. M. Gammon¹

AFFILIATIONS

¹School of Engineering, University of Warwick, Coventry CV4 7AL, United Kingdom

²Department of Physics, University of Warwick, Coventry CV4 7AL, United Kingdom

³Dynex Semiconductor Ltd., Lincoln LN6 3LF, United Kingdom

⁴Department of Materials Science and Chemical Engineering, Stony Brook University, Stony Brook, New York 11794, USA

^{a)}Author to whom correspondence should be addressed: a.renz@warwick.ac.uk

ABSTRACT

Molybdenum (Mo)/4H-silicon carbide (SiC) Schottky barrier diodes have been fabricated with a phosphorus pentoxide (P₂O₅) surface passivation treatment performed on the SiC surface prior to metallization. Compared to the untreated diodes, the P₂O₅-treated diodes were found to have a lower Schottky barrier height by 0.11 eV and a lower leakage current by two to three orders of magnitude. Physical characterization of the P₂O₅-treated Mo/SiC interfaces revealed that there are two primary causes for the improvement in electrical performance. First, transmission electron microscopy imaging showed that nanopits filled with silicon dioxide had formed at the surface after the P₂O₅ treatment that terminates potential leakage paths. Second, secondary ion mass spectroscopy revealed a high concentration of phosphorus atoms near the interface. While only a fraction of these are active, a small increase in doping at the interface is responsible for the reduction in barrier height. Comparisons were made between the P₂O₅ pretreatment and oxygen (O₂) and nitrous oxide (N₂O) pretreatments that do not form the same nanopits and do not reduce leakage current. X-ray photoelectron spectroscopy shows that SiC beneath the deposited P₂O₅ oxide retains a Si-rich interface unlike the N₂O and O₂ treatments that consume SiC and trap carbon at the interface. Finally, after annealing, the Mo/SiC interface forms almost no silicide, leaving the enhancement to the subsurface in place, explaining why the P₂O₅ treatment has had no effect on nickel- or titanium-SiC contacts.

© 2020 Author(s). All article content, except where otherwise noted, is licensed under a Creative Commons Attribution (CC BY) license (<http://creativecommons.org/licenses/by/4.0/>). <https://doi.org/10.1063/1.5133739>

I. INTRODUCTION

SiC is the most mature among the wide bandgap semiconductor materials. Due to the higher operating temperature, the lower specific on-resistance $R_{SP,ON}$, and the higher critical electric field, SiC devices are more suitable to operate in high power, high voltage, and high temperature applications than their silicon (Si) counterparts.¹ Since commercial SiC devices first became available in 2001, unipolar devices such as Schottky barrier diodes (SBDs) and metal-oxide-semiconductor field-effect transistors (MOSFETs) have been highly competitive in the power device market in the blocking voltage range of 600–1700 V, offering fast, low loss switching compared to Si insulated gate bipolar transistors (IGBTs) in this voltage range.² This, in turn, enables compact power converter solutions, opening up a wide application space in the automotive, industrial machines, and harsh

environment sectors.³ The SBD remains the most widely adopted and the most mature SiC device, yet it continues to improve. Commercial device designs almost universally employ junction barrier Schottky (JBS) architectures, p+ implantations beneath the Schottky metal helping to minimize reverse leakage and increase the surge current capability by shifting the peak electric field down to the p-n interface, away from the surface.^{4,5}

Improvements to the SiC SBD have focused on the choice of the Schottky contact metal, which governs the Schottky barrier height (SBH) at the metal/semiconductor interface.^{5–8} Until recently, SiC suppliers have opted for titanium (Ti) and titanium-silicides over nickel (Ni) and nickel-silicides as the Schottky contact metal, resulting in a low SBH and hence minimal turn-on voltage, due to its lower work function compared to Ni

($\phi_{\text{Ti}} = 4.33 \text{ eV}$ and $\phi_{\text{Ni}} = 5.04 - 5.35 \text{ eV}^9$). However, in the last five years, there has been research and development of molybdenum (Mo) Schottky contacts,^{8,10-12} which have a similar work function ($\phi_{\text{Mo}} = 4.36 - 4.95 \text{ eV}^9$) but a significantly higher melting point. In particular, Infineon integrated MoN contacts¹² into their 6th generation of SiC SBDs,^{13,14} which was reported to lower the SBH to 0.86 eV, resulting in even lower turn-on voltage at the expense of increased reverse leakage currents.¹³ Elsewhere however, the Mo/SiC interface was reported to have a barrier height as high as 1.28 eV by Bonyadi *et al.*,¹⁵ while in Latreche *et al.*¹⁶ and Lee *et al.*,¹⁷ it is 1.01 eV, with a very low ideality factor over a wide temperature range. The authors have previously reported SBH values between 1.27 eV and 1.43 eV.¹⁸

Surface passivation treatments prior to metal deposition have been shown^{16,18,19} to improve the electrical characteristics of the final diode. In Lee *et al.*,¹⁷ prior to the deposition of Ni, a postoxidation anneal (POA) in nitrous oxide (N_2O) ambient at 1000 °C for 2 h, before the removal of the grown oxide, resulted in both a tighter distribution of ideality factors across the measured SBDs and a significant reduction of leakage current densities.

Similar passivation treatments, including annealing in hydrogen, nitrogen, nitrous oxide, or argon ambient, annealing in phosphorous-containing ambients as well as boron incorporations have been employed in metal-oxide-semiconductor (MOS) structures on SiC in an attempt to reduce the density of interface states near the silicon dioxide (SiO_2)/SiC interface.¹⁹⁻²³ Among these methods, annealing in N_2O ambient has been found to be the most effective technique.²⁴ However, recent reports on the impact of phosphorus pentoxide (P_2O_5) depositions as a surface passivation for SBDs and MOSFETs^{18,25-27} have shown an improvement both in leakage current densities for SBDs and in channel mobility for transistors. As this treatment also improved the on-state performance of the measured devices, the benefits of nitridation prior to metallization of SBDs were exceeded. Hence, it has been shown that pretreatments of SBDs have the potential to minimize the disadvantages of using anode metals with low barrier heights.

In this paper, we investigate the impact of surface passivation treatments on both the SiC surface and the Mo/SiC Schottky interface. The passivation treatments not only focus on P_2O_5 deposition but also include the growth of oxide layers in O_2 and N_2O ambients. After these grown or deposited layers were removed, a Mo Schottky contact metal was deposited. The fabricated SBDs were compared to those on untreated (control) surfaces and analyzed electrically using forward and reverse I-V characteristics. Having identified improvements to the diodes that underwent a P_2O_5 passivation treatment, including significantly reduced leakage current, these and the control samples are analyzed using x-ray photoelectron spectroscopy (XPS), secondary ion mass spectroscopy (SIMS), transmission electron microscopy (TEM), atomic force microscopy (AFM), scanning electron microscopy (SEM), and synchrotron X-ray topography to identify the physical parameters that explain the electrical improvements.

II. EXPERIMENTAL PROCEDURE

Mo/SiC Schottky diodes were fabricated to analyze the effect of different passivation treatments on the turn-on and reverse

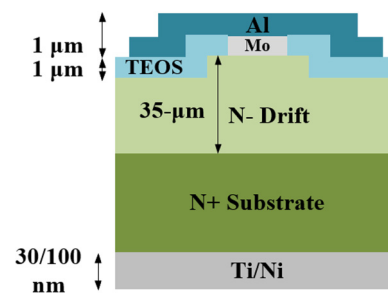


FIG. 1. Cross-sectional view of the fabricated Schottky barrier diodes with Mo as the Schottky contact metal. The Schottky contact area is $4.39 \times 10^{-4} \text{ cm}^2$.

leakage current levels. These were fabricated using highly *n*-type (nitrogen-doped), 4° off-axis 4H-SiC substrates supplied by Dow Corning, on which a lightly doped ($1 \times 10^{15} \text{ cm}^{-3}$) 35 μm epitaxial layer was grown. These starting wafers were diced into $14 \times 14 \text{ mm}^2$ chips and cleaned using a standard RCA 1/HF (10%)/RCA 2/HF (10%) process. Subsequently, one of three passivation routines were applied to the SiC samples:

1. The deposition of P_2O_5 in a tube furnace at 1000 °C for 2 h, the samples having been mounted on a carrier wafer and placed in front of a silicon diphosphate (SiP_2O_7) source wafer (the P_2O_5 treatment).
2. Thermal oxidation in an $\text{Ar}:\text{O}_2$ (4 slm:1 slm) ambient at 1400 °C for 4 h (henceforth referred to as the O_2 treatment).
3. Thermal oxidation in an $\text{Ar}:\text{N}_2\text{O}$ (4 slm:1 slm) ambient at 1300 °C for 4 h (the N_2O treatment).

A fourth set of control samples was fabricated in parallel, which underwent no passivation treatment. Next, all the treated samples were cleaned in dilute HF (10%) to remove the oxide layers before the individual active areas of Schottky diodes were defined and mesa-isolated by dry etch. For device insulation, a 1 μm thick SiO_2 layer was deposited by low pressure chemical vapor deposition (LPCVD) using tetraethyl orthosilicate (TEOS) as a precursor, covering the active areas before the contact formation. Ti(30 nm)/Ni (100 nm) ohmic contacts were then formed on the backside of the samples after a rapid thermal anneal at 1000 °C for 2 min in Ar (5 slm) ambient. Schottky contacts were then formed by opening a window in the thick SiO_2 layer and evaporating 100 nm of Mo before annealing them at 500 °C in Ar (5 slm) ambient. Finally, a 1 μm thick Al metal overlay was evaporated on top of the die, which serves as a field plate. A cross section of the fabricated final device structure can be found in Fig. 1.

Several chips have been fabricated across a number of different wafers from the batch. The results presented here were repeatable across the die from the same and different wafers.

III. RESULTS

A. Current voltage (I-V)

The rectifying characteristics of all the diodes were characterized via I-V measurements at room temperature using a Keysight

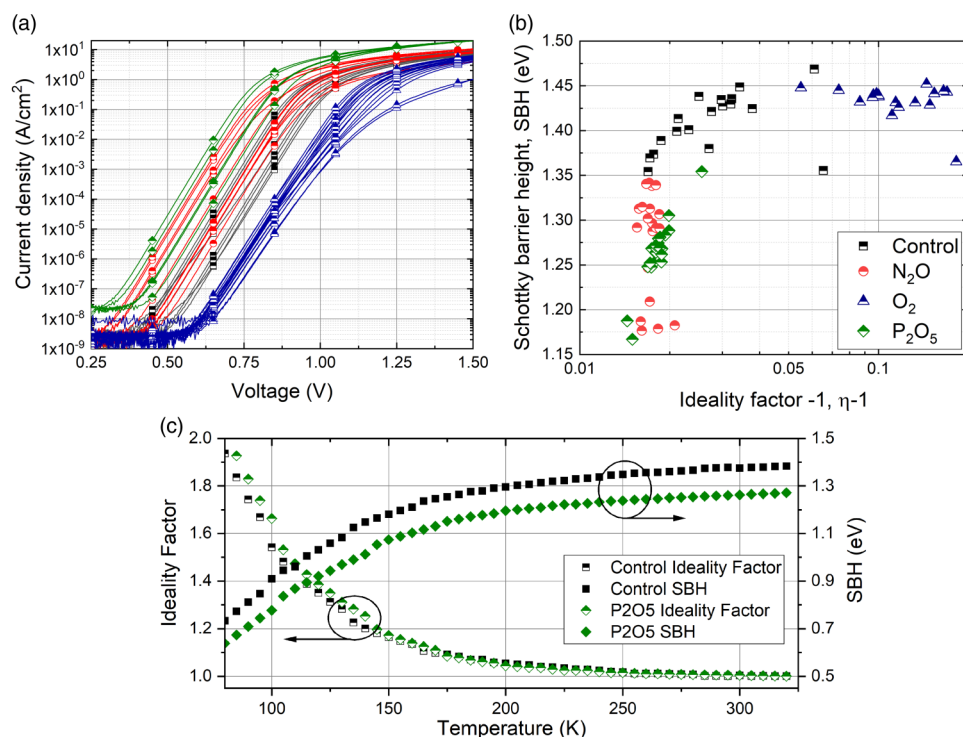


FIG. 2. Typical on-state I-V characteristics (a) of the Schottky diodes, measured at 22 °C. SBH and ideality factors (b) for these diodes at room temperature as well as from 80 to 320 K (c) for a typical control and P₂O₅-treated diode.

B1505A parameter analyzer and a semiprobe semiautomatic probe station. On-state parameters were then extracted from the on-state characteristics, assuming that thermionic emission^{2,6} was the governing conduction mechanism at the Schottky interface. The ideality factor (η) and SBH were measured between leakage current densities of 1×10^{-7} and 1×10^{-3} A cm⁻². A typical set of on-state characteristics (at room temperature) for the Mo/SiC diodes are shown in Fig. 2(a), as well as their barrier heights and ideality factors (plotted as $\eta - 1$) in Fig. 2(b) for at least 15 different SBDs of each type. All the diodes had very low values of η , confirming that thermionic emission is the dominant current transport mechanism.⁶ Without any surface treatment, the control samples had a relatively wide spread of SBH and η , which averaged at 1.41 eV and 1.03, respectively (Fig. 2). A summary of the extracted electrical parameters is shown in Table I.

From this baseline, the O₂ surface treatment appears to have worsened the electrical characteristics, resulting in a higher average SBH of 1.43 eV and η of 1.09, while there remains a wide spread of the results. On the contrary, the SBH was significantly lowered by applying the N₂O and P₂O₅ treatments, with average values of 1.28 eV and 1.27 eV, respectively. These diodes also had extremely low η , all below 1.02, and a tight, repeatable distribution.

Figure 2(c) shows the ideality factor and the SBH taken from 80 to 320 K, for a typical control diode and P₂O₅-treated diode. Both diodes follow typical trends, explained elsewhere,^{2,6,7} with η increasing and SBH decreasing at low temperatures. There is little difference in the ideality factor, which remains below 1.1 until 175 K for both diodes. However, it can be seen that the room

temperature offset in the SBH of 0.10–0.13 eV is maintained across the temperature range.

The most significant outcome of this study is shown in Fig. 3, which summarizes the leakage current density (at $V_R = 500$ V) of at least 60 diodes per treatment. Despite the reduction in SBH demonstrated in Fig. 2 and Table I for the P₂O₅-treated diodes, these can be seen to give the lowest leakage current levels, with a median value of 1.5×10^{-6} A cm⁻², three orders of magnitude lower than the control diodes. This is contrary to the expectation that the reduced SBH (and hence a lower turn-on voltage) will result in an increased leakage, as happened when Infineon moved from Ti to Mo.^{13,14}

In Bonyadi *et al.*,¹⁵ these Mo/SiC diodes were compared to Ni and Ti SiC diodes that underwent the same pretreatments. These results showed that a P₂O₅-treated Mo/SiC diode had a SBH equivalent to Ti, but a leakage current lower than any Ni diode,

TABLE I. Summary of measured ideality factors, barrier heights, and reverse leakage currents of the as-grown and treated samples. All measurements were carried out at room temperature. Mean values are provided with standard deviations.

Sample	Schottky barrier height (eV)	Ideality factor	Reverse leakage current at -500 V (A cm ⁻²)
Control	1.38 ± 0.08	1.05 ± 0.09	$1.47 \times 10^{-2} \pm 3.01 \times 10^{-2}$
O ₂ treated	1.43 ± 0.04	1.09 ± 0.04	$2.34 \times 10^{-3} \pm 3.56 \times 10^{-3}$
N ₂ O treated	1.28 ± 0.06	1.02 ± 0.01	$4.07 \times 10^{-3} \pm 9.28 \times 10^{-3}$
P ₂ O ₅ treated	1.27 ± 0.03	1.02 ± 0.01	$2.12 \times 10^{-5} \pm 6.13 \times 10^{-5}$

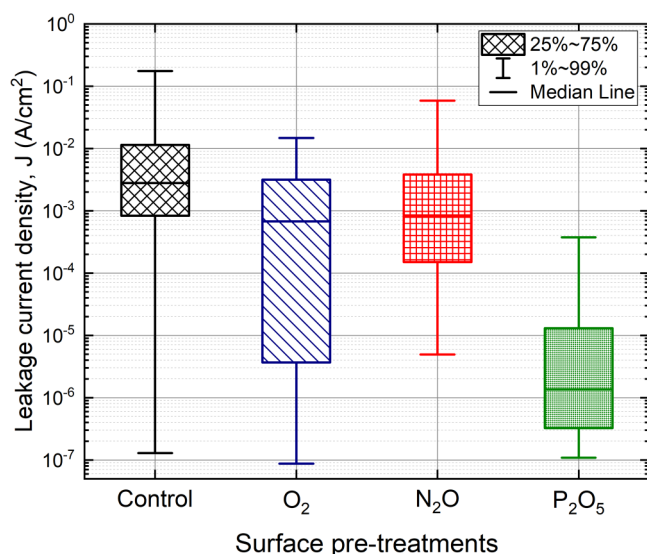


FIG. 3. Diode leakage current characteristics at $V_R = 500$ V, measured at 22°C . Median values are represented due to the logarithmic scale.

thus combining the benefits of both low- and high-SBH metals. Furthermore, the Mo diodes were the only diodes to undergo any significant leakage current reduction after any of the pretreatments. To investigate the mechanisms by which the P_2O_5 treatment improves the diode characteristics, a series of physical analyses were carried out.

B. Surface chemistry study using X-ray photoelectron spectroscopy (XPS) and secondary ion mass spectroscopy (SIMS)

X-ray photoelectron spectroscopy (XPS) characterization was performed in order to investigate the physical and chemical properties of the SiC surface after removal of the previously grown or deposited oxides. Samples were prepared using the oxide growth and deposition procedures described above, with the oxides being removed in HF (10%) solution afterwards. The samples were then immediately loaded into a Kratos Axis Ultra DLD XPS system. The samples were illuminated with Al $K\alpha$ X-rays (1486.6 eV), the spectrometer work function was calibrated using polycrystalline Ag foil prior to the experiments, and the spectra were analyzed at takeoff angles (ToA) of 90° and 15° , giving 3λ depths of 10 nm and <3 nm, respectively. High-resolution core spectra were taken for Si 2p, C 1s, O 1s, P 2p, and N 1s, and the data were analyzed using the CasaXPS software package, employing Shirley backgrounds and Voigt (Gaussian-Lorentzian) line shapes. The Si 2p and C 1s of the untreated sample spectra are shown in Figs. 4(a) and 4(b). All spectra are shown for a 90° ToA.

Due to the presence of adventitious carbon in XPS, carbon clusters cannot be quantified directly from the XPS spectra. In order to analyze the effect of surface treatments on carbon clusters, the Si:C stoichiometry of the surface is extracted using the relative atomic

concentration of SiC components in the C 1s and Si 2p spectra. An overview of the obtained Si:C ratios can be seen in Fig. 4(c).

For the 90° ToA, the results were close to stoichiometric. The control sample showed stoichiometry closest to 1.0 and, consistent with the carbon cluster model, the O_2 treatment gave a 4.3% carbon-rich surface and the N_2O treatment restored stoichiometry. The P_2O_5 treatment gave a 2.4% silicon enrichment, showing clear evidence of a surface modification and indicating that silicon, or possibly SiO_2 , may have a role in improved diode performance. For the 15° ToA, the O_2 and N_2O treatments gave carbon enrichments of 13% and 20%, while P_2O_5 gave the lowest carbon enrichment of 7.5%. The 15° ToA quantification was more significantly affected by adventitious carbon, which may have influenced the analysis, but it is also more sensitive to the surface composition, suggesting that the surface may be more carbon-rich than the 10 nm below it. For both measurements, the P_2O_5 treatment has shown to combat carbon enrichment.

The P 2p spectrum of the P_2O_5 -treated sample is shown in Fig. 4(d) and confirms the presence of phosphorus pentoxide following the P_2O_5 treatment.^{28–30} This shows that traces of P_2O_5 can be found near the surface even after the removal of the oxide via HF. This peak was not observed for any of the other samples. Secondary ion mass spectrometry (SIMS) was used to further confirm the presence of phosphorus after the P_2O_5 treatment and metallization and to investigate its depth distribution. One sample was prepared using the P_2O_5 treatment and Mo deposition, as described above. SIMS was carried out using Si, C, and P+ matrix markers at a high resolution (<1 nm) near the Mo/SiC interface (100–200 nm). Figure 5 shows the SIMS spectra. Phosphorus concentrations of up to $1.5 \times 10^{19} \text{ cm}^{-3}$ could be detected at the Mo/SiC interface.

This surface chemistry study has shown, using XPS, that a phosphorous deposition (P_2O_5) process in N_2 ambient does not lead to carbon enrichment at the interface, unlike the O_2 treatment and the N_2O treatment at a shallow probing depth. Furthermore, both XPS and SIMS results show that phosphorus remains are found after HF etching and postmetallization.

C. Surface morphology study using atomic force microscopy (AFM) and scanning electron microscopy (SEM)

AFM and SEM images were taken for a P_2O_5 -treated sample and an untreated control sample. A Bruker Icon AFM was used in a peakforce tapping mode. The probe tip was made of Si on a nitride lever. The scan area of the presented images is $5 \times 5 \mu\text{m}^2$. Four scans were taken for both samples across different positions on the chip with little difference between the regions. For the SEM investigation, the same samples were investigated in a Zeiss SUPRA 55-VP FEGSEM at an accelerating voltage of 15 kV. Two scans were taken for both samples, with representative images shown in Fig. 6.

As a result of the AFM images, RMS roughness values below 1 nm were measured for both samples, with average values of 351 pm for the control sample and 711 pm for the P_2O_5 -treated sample. The P_2O_5 -treated sample shows clear circular features with a density of approximately $5 \times 10^9 \text{ cm}^{-2}$, as shown in Fig. 7(a). Their size and shape vary across the sample, with widths between

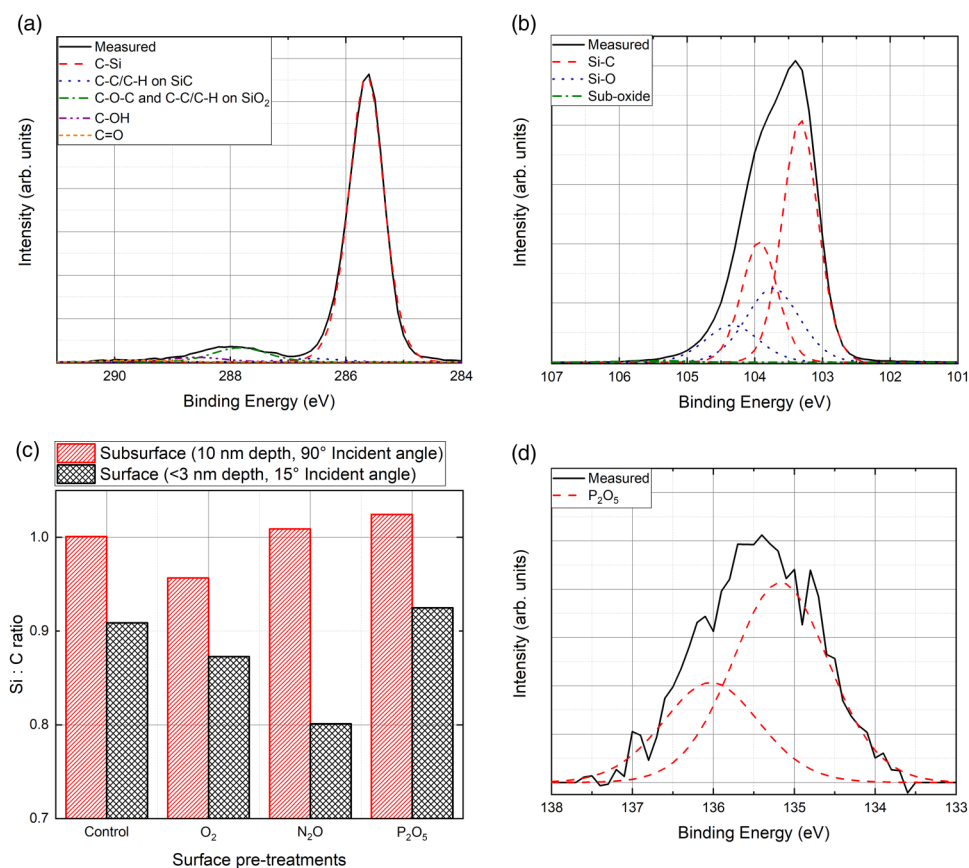


FIG. 4. XPS data and fits for the (a) C 1s region, (b) Si 2p region without surface treatment, (c) P 2p region showing a P₂O₅ peak for the P₂O₅-treated sample, and (d) Si:C ratio of the investigated samples at different surface depths.

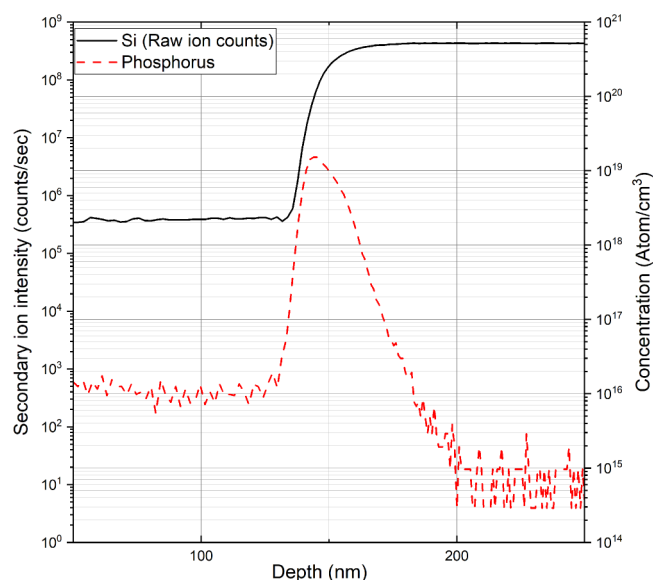


FIG. 5. SIMS results for the P₂O₅-treated sample.

70 and 200 nm and depths ranging from 1 to 3 nm, although the measurable depth was limited by the AFM tip.

In the untreated sample, normal SiC surface steps are clearly visible, while the circular surface features of visible post-P₂O₅ treatment are also faintly visible, though not as deep pits, but rather very small peaks. The same surface features were not seen in the post-N₂O/O₂ treatment. The SEM showed the extent of these defects over a wider area. Figure 6 shows the P₂O₅-treated and control surfaces at 1 μ m and 200 nm fields of view, respectively.

With the AFM micrographs, the difference between the control and P₂O₅-treated surfaces is visible. The P₂O₅-treated surface shows the same feature sizes and shapes as the AFM micrographs, with similar densities of $5.5 \times 10^9 \text{ cm}^{-2}$ and a slightly rougher surface. The surface morphology study has shown that the P₂O₅ treatment has induced a high intensity of surface features, not seen in the control sample.

D. Cross-sectional analysis using transmission electron microscopy (TEM)

Cross-sectional TEM specimens of the control and P₂O₅-treated Mo/SiC SBDs were prepared using a focused ion beam. The interface of these devices was observed in either a JEOL 2100 TEM or a JEOL ARM 2000F TEM. Energy-dispersive x-ray

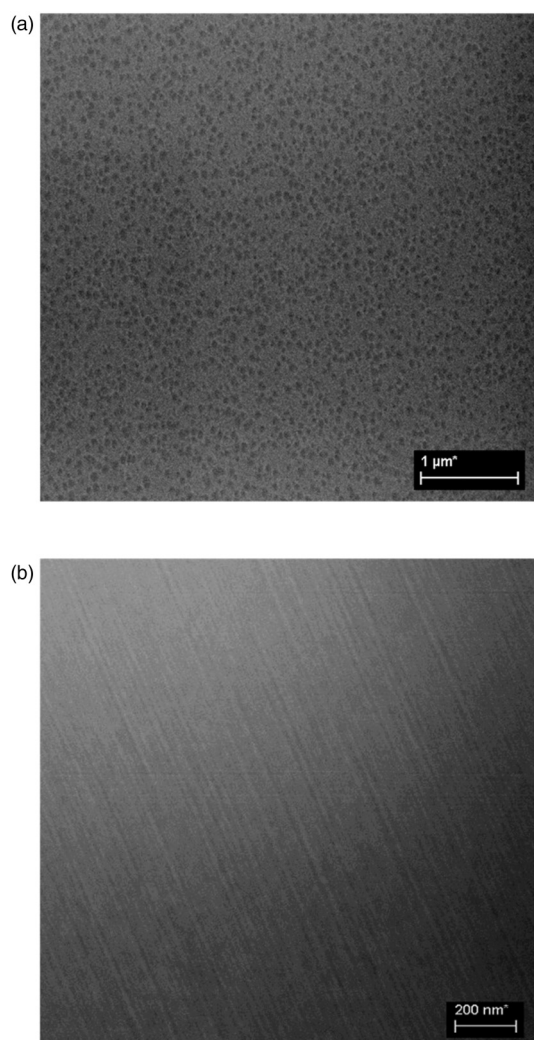


FIG. 6. SEM images of (a) a P_2O_5 -treated sample and (b) an untreated control with a $1\ \mu\text{m}$ and $200\ \text{nm}$ scan size, respectively.

analysis (EDX) was performed in the JEOL ARM200F equipped with a $100\ \text{mm}^2$ Oxford Instruments windowless EDX detector.

In places along the P_2O_5 -treated interface, such as that shown in Fig. 8(a), features can be seen which propagate approximately $10\ \text{nm}$ into the SiC. These are distributed nonuniformly across the observed interface, with region widths varying from 80 to $120\ \text{nm}$.

EDX mapping results confirm that these are amorphous features with an increased oxygen concentration, which are most likely formed due to the incorporation of oxygen during the P_2O_5 treatment, since no such features and oxygen concentrations were found in the untreated SiC sample.

The oxide in these pits, therefore, remains after the HF dip that removed the P_2O_5 layer.

In contrary, the untreated control sample shows a uniform interface, with an interfacial region less than $2\ \text{nm}$ thick.

E. Substrate and epitaxial defect characterization using synchrotron x-ray topography

To investigate a potential connection between the high density ($5 \times 10^9\ \text{cm}^{-2}$) of surface defects and typical SiC defects—basal plane dislocations (BPDs), threading edge dislocations (TEDs), and threading screw dislocations (TSDs)—in the underlying epitaxial layer and substrate, synchrotron x-ray topographs were taken from untreated and treated (all three surface treatments) samples that had previously undergone SEM and AFM analyses. The imaging was carried out at beamline 1-BM at Advanced Photon Source, Argonne National Laboratory, USA. To image all dislocations in the substrate and epitaxial layers, $11\bar{2}0$ reflections were recorded. For stacking fault detection, $10\bar{1}0$ and $10\bar{1}1$ reflections were recorded. Grazing incidence angle scans (resulting in a penetration depth of $35\ \mu\text{m}$) were also performed along the $11\bar{2}8$ plane to detect threading dislocations and BPDs in the epitaxial layer. A grazing incidence angle scan of the untreated control sample revealed that no BPDs were observed except around a 3C inclusion, which indicates that they are all converted to TEDs during the epigrowth. No deflected dislocations were observed for the control sample. For the P_2O_5 -treated sample, some BPDs were seen and this sample showed the highest density of TEDs measured across all samples. No stacking faults could be observed for any of the analyzed samples. An overview of the measured defect densities of all investigated samples can be seen in Table II. There is some significant difference between the values extracted, but it is expected that most of these differences come from the varying locations of the chips from across the wafer. All these bulk defect densities are on average 5 orders of magnitude lower than the measured surface feature density of $5 \times 10^9\ \text{cm}^{-2}$. This suggests that the observed features on AFM and SEM micrographs are not related to defects that originate in the bulk or epitaxy.

IV. DISCUSSION

The electrical measurements of the P_2O_5 -treated diodes revealed a reduction in the off-state leakage of the Mo/SiC SBDs of 2–3 orders of magnitude, compared to those that had not been treated. Furthermore, these devices had a SBH $0.11\ \text{eV}$ lower than the untreated control samples, which appears to defy the logical leakage current vs turn-on voltage trade-off dictated by the Schottky barrier height. It is worth noting that the leakage of these Mo diodes is also lower than identical Ni/SiC diodes produced previously,¹⁵ despite a barrier height of $>0.3\ \text{eV}$ being lower. At the same time, both the ideality factor of the devices and the uniformity of the results were improved by the P_2O_5 treatment, suggesting an overall improvement in the homogeneity of the metal-semiconductor interface.

AFM images, shown in Fig. 7, and TEM images, shown in Fig. 8, revealed that the P_2O_5 treatment has a physical impact on the SiC surface, creating “nanopits” that are $3\text{--}10\ \text{nm}$ deep and wide. Despite the wafer having undergone a HF dip to remove the oxide left on the surface after the pretreatments, EDX analysis suggests that a significant quantity remained within the surface pits. Despite evidence of phosphorous at the surface from SIMS, it was not possible to identify phosphorous in the nanopits within the detection limit of EDX.

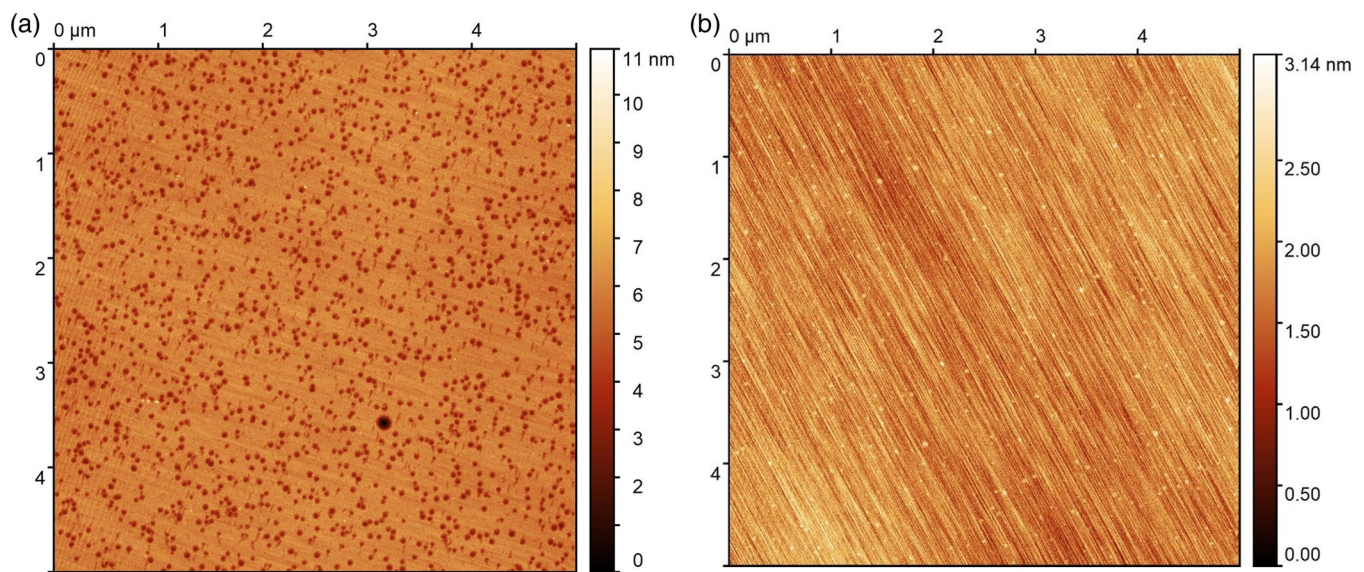


FIG. 7. AFM images of (a) an untreated control surface and (b) a P_2O_5 -treated sample with a $5 \times 5 \mu m^2$ scan size.

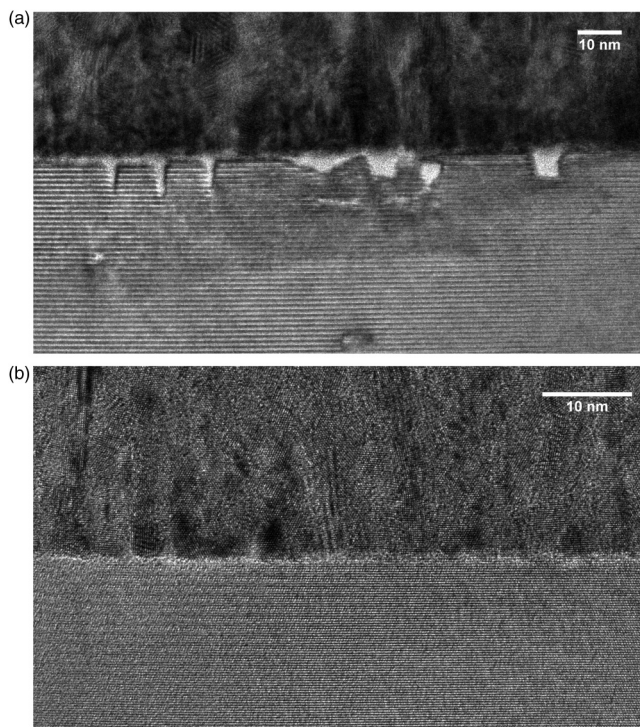


FIG. 8. HRTEM images of the Mo/SiC interface of (a) the P_2O_5 -treated and (b) the untreated control SBD.

The oxide-filled nanopits are believed to have the biggest impact on the electrical characteristics of the device. From synchrotron x-ray topography analysis, it is evident that their high density ($5 \times 10^9 \text{ cm}^{-2}$) does not correlate with any identifiable bulk or epitaxial defects, which means that the nanopits observed here are different from other nanopits³¹ that have been shown to be the source of a high leakage forming at the surface of threading dislocations.

Regardless of their origin, the termination of the surface features, which are barely visible on the AFM scan of the control sample, has the effect of homogenizing the interface, given that current is prevented from passing through these areas. Any source of inhomogeneity at a Schottky interface causes a degradation of the diode's I-V characteristics, with dirt, defects, and grain boundaries all having been linked to an increase in the distribution of SBH at an interface, leading to a degradation of I-V characteristics.⁵⁻⁷ The electrical results shown in Table I confirm that the termination of these defective areas results in a set of diodes with minimal spread in SBH between devices.

It is proposed, therefore, that the oxide-terminated nanopits are a source of leakage within the control samples, yet they are terminated in the P_2O_5 -treated diodes. The leakage may arise either by (1) being a region of low SBH or (2) by simply being an imperfection, an area in which the electric field is higher locally than across the rest of the interface.

If case 1 were true and areas of low SBH were being terminated, one might expect the average SBH of the P_2O_5 -treated diodes, obtained by I-V analysis, to be greater than that of the untreated control samples. Contrary to this, the barrier height of the P_2O_5 -treated diodes was, on average, 0.11 eV lower. However, this

TABLE II. Summary of measured defect densities of the as-grown and treated samples.

Sample	BPD (cm ⁻²)	TED (cm ⁻²)	TSD (cm ⁻²)
Control	814	2378	1202
O ₂ treated	3085	460	690
N ₂ O treated	1618	1790	1355
P ₂ O ₅ treated	3045	12 122	383

does not eliminate this possibility. SIMS and XPS analysis both showed that a significant amount of phosphorous ($>1 \times 10^{19} \text{ cm}^{-3}$) is present at the interface, left over from the removed P₂O₅ layer. Without any high temperature activation, only a small fraction of these phosphorous atoms will have become active dopants. Indeed, basic calculations relating N_D to the Fermi level position³² confirm that an increase in active dopants from $1 \times 10^{15} \text{ cm}^{-3}$ in the control diodes to $7 \times 10^{16} \text{ cm}^{-3}$ in the P₂O₅ diodes would result in the Fermi level being 0.11 eV closer to the conduction band and hence the same reduction in barrier height. Despite the increase in doping, E_{00} calculations³² confirm that the dominant conduction mechanism at $7 \times 10^{16} \text{ cm}^{-3}$ will remain thermionic emission and not thermionic field emission. This theory is supported by the very low ideality factors in the P₂O₅ diodes, which would not be the case if the doping was high enough for thermionic field emission to dominate. Therefore, the increase in subsurface doping, combined with the homogenization of the barrier height after the oxide termination of surface defects, could explain the reduction of the barrier, while simultaneously decreasing leakage.

In the case of the N₂O treatment, the leakage current was not improved, but the SBH and ideality factors were reduced. For the O₂ treatment, no improvement of the electrical characteristics was seen. Both of these treatments are different from the deposited P₂O₅ treatment, in that they consume the top few nanometers of SiC while forming an oxide. XPS results confirm that, in the case of O₂, the stoichiometry of the SiC subsurface was poor, with carbon enrichment near the interface. However, N₂O restored the stoichiometry at the deep probing depth, but left a carbon-rich surface at a shallow probing depth. This is consistent with the carbon cluster model, where thermal oxidation treatments trap carbon beneath the oxide and, in turn, cause low channel mobility in SiC MOSFETs. In contrast, the P₂O₅ treatment retained a Si-rich interface, principally because the deposited layer does not consume the SiC but fills the previously described nanopits. However, the previously described *n*-type doping of the interface beneath the contact may have occurred in the N₂O sample, explaining its improved SBH and ideality factor.

Finally, these subtle changes in the contact subsurface can only occur because almost no silicide is formed after a Mo/SiC interface is annealed. This is due to the high melting temperature of Mo and has the result of preserving the monolayers of treated SiC beneath the interface, as seen in the TEM images of Fig. 8. This explains why the P₂O₅ treatment has no effect on other metals, such as Ti and Ni, which do form significant silicides at the interface. This leads to the question as to whether this treatment will work on other refractory metals, such as tungsten, niobium,

and tantalum. Furthermore, this was a study performed on SiC wafers from one supplier, with 35 μm of epitaxy. Whether the P₂O₅ treatment will have the same beneficial effect on wafers from other suppliers, other epitaxy thicknesses, and at SiC interfaces with other refractory metals is still a work in progress.

V. CONCLUSION

A P₂O₅ surface passivation treatment prior to metallization has demonstrated a significant improvement in the performance of Mo/SiC Schottky barrier diodes. The electrical characterization showed that P₂O₅-treated diodes have a leakage current two orders of magnitude lower than untreated control diodes, a reduction in the Schottky barrier height of 0.11 eV (and hence lower turn-on voltage), and a small improvement in the ideality factor. The P₂O₅ treatment appears to have two effects on the contact subsurface. First, the leakage is likely improved due to the formation of oxide-filled nanopits, witnessed in AFM and TEM scans, which terminate potential leakage paths from imperfections at the SiC surface and homogenize the interface. Second, the barrier is lowered due to a phosphorous-rich region below the contact, which increases the *n*-type doping and lowers the SBH. Finally, the enhancement of this subcontact region is only possible because there is no silicide formed at the Mo/SiC interface, which would otherwise consume the top few nanometers of SiC (as in Ti and Ni). These results offer both increased performance of SiC SBDs and present opportunities to improve SBD performance and SiC surface passivation.

ACKNOWLEDGMENTS

The work presented in this paper was carried out as part of the Engineering and Physical Sciences Research Council (EPSRC) under Project Nos. EP/P017363/1 and EP/R00448X/1. We gratefully acknowledge the support of Dr. Mark Crouch and Corinne Maltby of the University of Warwick clean room staff for their support during device fabrication. Topographs were recorded using the resources of the Advanced Photon Source (Beamline 1-BM), a U.S. DOE Office of Science User Facility operated for the DOE Office of Science by the Argonne National Laboratory under Contract No. DE-AC02-06CH11357.

REFERENCES

- ¹T. Kimoto and J. A. Cooper, *Fundamentals of Silicon Carbide Technology: Growth, Characterization, Devices and Applications* (John Wiley & Sons, New York, 2014).
- ²F. Roccaforte, P. Fiorenza, G. Greco, R. L. Nigro, F. Giannazzo, F. Iucolano, and M. Saggio, "Emerging trends in wide band gap semiconductors (SiC and GaN) technology for power devices," *Microelectron. Eng.* **187–188**, 66–77 (2018).
- ³X. She, A. Q. Huang, O. Lucia, and B. Ozpineci, "Review of silicon carbide power devices and their applications," *IEEE Trans. Ind. Electron.* **64**, 8193–8205 (2017).
- ⁴D. Navarro, F. Herrera, H. Zenitani, M. Miura-Mattausch, N. Yorino, H. J. Mattausch, M. Takusagawa, J. Kobayashi, and M. Hara, "Compact modeling of SiC Schottky barrier diode and its extension to junction barrier Schottky diode," *Jpn. J. Appl. Phys.* **57**, 04FR03 (2018).
- ⁵F. Roccaforte, G. Brezeanu, P. Gammon, F. Giannazzo, S. Rascunà, and M. Saggio, and "Schottky contacts to silicon carbide: Physics, technology and applications," in *Advancing Silicon Carbide Electronics Technology, I: Metal*

Contacts to Silicon Carbide: Physics, Technology, Applications (Materials Research Forum LLC, 2018).

⁶R. Tung, "Electron transport at metal-semiconductor interfaces: General theory," *Phys. Rev. B* **45**, 13509 (1992).

⁷P. Gammon, A. Pérez-Tomás, V. Shah, O. Vavasour, E. Donchev, J. Pang, M. Myronov, C. Fisher, M. Jennings, D. Leadley, and P. A. Mawby, "Modelling the inhomogeneous SiC Schottky interface," *J. Appl. Phys.* **114**, 223704 (2013).

⁸Z. Ouenoughi, S. Toumi, and R. Weiss, "Study of barrier inhomogeneities using I-V-T characteristics of Mo/4H-SiC Schottky diode," *Physica B* **456**, 176–181 (2015).

⁹H. B. Michaelson, "The work function of the elements and its periodicity," *J. Appl. Phys.* **48**, 4729–4733 (1977).

¹⁰R. Gharbi, K. Shili, M. Ben Karoui, M. Fathallah, and S. Ferrero, "Barrier height evolution in a non-uniform interface of Ti or Mo Schottky diodes based on 4H-SiC," *Int. J. Electron. Lett.* **4**, 367–375 (2016).

¹¹T. Zhang, C. Raynaud, and D. Planson, "Measure and analysis of 4H-SiC Schottky barrier height with Mo contacts," *Eur. Phys. J. Appl. Phys.* **85**, 10102 (2019).

¹²L. Stöber, J. P. Konrath, F. Patocka, M. Schneider, and U. Schmid, "Controlling 4H-SiC Schottky barriers by molybdenum and molybdenum nitride as contact materials," *IEEE Trans. Electron. Devices* **63**, 578–583 (2015).

¹³R. Rupp, R. Elpelt, R. Gerlach, R. Schömer, and M. Draghici, "A new SiC diode with significantly reduced threshold voltage," in *2017 29th International Symposium on Power Semiconductor Devices and IC's (ISPSD)* (IEEE, 2017), pp. 355–358.

¹⁴Infineon, CoolSiC™ Schottky diode 650V G5 and G6, improved efficiency and price performance, see <https://www.infineon.com/cms/en/product/power/silicon-carbide-sic/cool-sic-schottky-diode/cool-sic-schottky-diode-650v-g5-and-g6/G6> (2017).

¹⁵Y. Bonyadi, P. M. Gammon, Y. K. Sharma, G. Baker, and P. A. Mawby, "An investigation into the impact of surface passivation techniques using metal-semiconductor interfaces," in *Materials Science Forum* (Trans Tech Publications, 2017), Vol. 897, pp. 443–446.

¹⁶A. Latreche, Z. Ouenoughi, and R. Weiss, "Temperature dependence of the inhomogeneous parameters of the Mo/4H-SiC Schottky barrier diodes," *Semicond. Sci. Technol.* **31**, 085008 (2016).

¹⁷D. Lee, C. Kim, H. Lee, S. Lee, H. Kang, H. Kim, H. K. Park, J. Heo, and H. J. Kim, "Improving the barrier height uniformity of 4H-SiC Schottky barrier diodes by nitric oxide post-oxidation annealing," *IEEE Electron Device Lett.* **35**, 868–870 (2014).

¹⁸A. B. Renz, V. A. Shah, O. Vavasour, Y. Bonyadi, G. Baker, F. Li, T. Dai, M. Walker, P. A. Mawby, and P. M. Gammon, "Surface effects of passivation within Mo/4H-SiC Schottky diodes through MOS analysis," in *Materials Science Forum* (Trans Tech Publications, 2019), Vol. 963, pp. 511–515.

¹⁹R. Ghandi, B. Buono, M. Domeij, R. Esteve, A. Schoner, J. Han, S. Dimitrijevic, S. A. Reshanov, C.-M. Zetterling, and M. Ostling, "Surface-passivation effects on

the performance of 4H-SiC BJTs," *IEEE Trans. Electron Devices* **58**, 259–265 (2010).

²⁰R. Pascu, F. Craciunoiu, M. Kusko, M. Mihaila, G. Pristavu, M. Badila, and G. Brezeanu, "SiO₂/4H-SiC interface states reduction by POCl₃ post-oxidation annealing," in *2015 International Semiconductor Conference (CAS)* (IEEE, 2015), pp. 255–258.

²¹D. Okamoto, M. Sometani, S. Harada, R. Kosugi, Y. Yonezawa, and H. Yano, "Improved channel mobility in 4H-SiC MOSFETs by boron passivation," *IEEE Electron Device Lett.* **35**, 1176–1178 (2014).

²²Z. Chen, Y. Xu, E. Garfunkel, L. C. Feldman, T. Buyuklimanli, W. Ou, J. Serfass, A. Wan, and S. Dhar, "Kinetics of nitrogen incorporation at the SiO₂/4H-SiC interface during an NO passivation," *Appl. Surf. Sci.* **317**, 593–597 (2014).

²³J.-L. Cantin, H. Von Bardeleben, Y. Ke, R. Devaty, and W. Choyke, "Hydrogen passivation of carbon Pb like centers at the 3C- and 4H-SiC/SiO₂ interfaces in oxidized porous SiC," *Appl. Phys. Lett.* **88**, 092108 (2006).

²⁴A. Siddiqui, H. Elgabra, and S. Singh, "The current status and the future prospects of surface passivation in 4H-SiC transistors," *IEEE Trans. Device Mater. Reliab.* **16**, 419–428 (2016).

²⁵Y. K. Sharma, A. C. Ahly, T. Isaacs-Smith, A. Modic, M. Park, Y. Xu, E. L. Garfunkel, S. Dhar, L. C. Feldman, and J. R. Williams, "High-mobility stable 4H-SiC MOSFETs using a thin PSG interfacial passivation layer," *IEEE Electron Device Lett.* **34**, 175–177 (2013).

²⁶Y. K. Sharma, A. C. Ahly, T. Issacs-Smith, X. Shen, S. T. Pantelides, X. Zhu, L. C. Feldman, J. Rozen, and J. R. Williams, "Phosphorous passivation of the SiO₂/4H-SiC interface," *Solid State Electron.* **68**, 103–107 (2012).

²⁷Y. K. Sharma, A. C. Ahly, T. Isaacs-Smith, A. Modic, Y. Xu, E. Granfukel, M. R. Jennings, C. Fisher, S. M. Thomas, P. A. Mawby, S. Dhar, L. C. Feldman, and J. R. Williams, "Thin PSG process for 4H-SiC MOSFET," in *Materials Science Forum* (Trans Tech Publications, 2014), Vol. 778, pp. 513–516.

²⁸B. V. R. Chowdari, K. L. Tan, W. T. Chia, and R. Gopalakrishnan, "X-ray photoelectron spectroscopic studies of molybdenum phosphate glassy system," *J. Non-Cryst. Solids* **119**, 95–102 (1990).

²⁹H. He, K. Alberti, T. L. Barr, and J. Klinowski, "ESCA studies of aluminophosphate molecular sieves," *J. Phys. Chem.* **97**, 13703–13707 (1993).

³⁰D. T. Clark, T. Fok, G. G. Roberts, and R. W. Sykes, "An investigation by electron spectroscopy for chemical analysis of chemical treatments of the (100) surface of *n*-type InP epitaxial layers for Langmuir film deposition," *Thin Solid Films* **70**, 261–283 (1980).

³¹T. Katsuno, Y. Watanabe, H. Fujiwara, M. Konishi, H. Naruoka, J. Morimoto, T. Morino, and T. Endo, "Analysis of surface morphology at leakage current sources of 4H-SiC Schottky barrier diodes," *Appl. Phys. Lett.* **98**, 222111 (2011).

³²S. M. Sze and K. K. Ng, *Physics of Semiconductor Devices* (John Wiley & Sons, New York, 2006).